

*Original Research*

# Emission Characteristics of CO and NO<sub>x</sub> from Tunnel Blast Design Models: a Comparative Study

Jihui Chen, Wenge Qiu\*, Partab Rai, Xufeng Ai

Key Laboratory of Transportation Tunnel Engineering, Ministry of Education, School of Civil Engineering,  
Southwest Jiaotong University, Chengdu, 610031, PR China

*Received: 28 January 2021*

*Accepted: 8 May 2021*

## Abstract

A large number of toxic gases such as carbon monoxide (CO) and nitrogen oxides (NO<sub>x</sub>) are produced from the blast models during the drill and blast tunneling excavation. However, the emission characteristics of blast design models have never been mentioned in previously published studies. To acquire the cleanest blast model and reduce environmental pollution, this paper for the first time compares the emission characteristics of CO and NO<sub>x</sub> from three traditional blast design models, i.e., NTNU, Swedish, and China models, which is the most used in tunneling. Firstly, the detailed blasting parameters of three models are put forward based on one certain 42.3m<sup>2</sup> cross-section tunnel. After that, the emission characteristics of each model is evaluated based on the indexes of total emission, emissions per area, and emission increment. Meanwhile, the tunnel face of the models is divided into four functional sections, i.e. cut zone, stoping zone, lifter zone, and contour zone to explore the influence of functional blastholes on gas emissions. Finally, these results indicate that the CO and NO<sub>x</sub> emissions of the China model are the least, followed by Swedish and NTNU models. And the total emissions are dominated by the stoping blastholes. Therefore, it is effective to reduce environmental pollution by adjusting the parameters of the stoping zone. This research can provide a reference for the tunnel engineers to design blast models to reduce environmental pollution.

**Keywords:** tunnel blast design model, CO emission, NO<sub>x</sub> emission, emission characteristics

## Introduction

The civil explosives are widely used in mining, extraction and construction industries, and play a great role in our production and life. The world production

of civil explosives has been increasing, which will increase to 16 million tonnes in 2018 [1]. And in drilling and blasting (D&B) tunnel, the extensive explosives are inevitably used. With the development of tunnel construction rapidly in China [2], the demand for explosives is also increasing. Although the use of explosives improves production efficiency and creates benefits for enterprises, there is a source of concern due to its associated environmental impact. On the one

---

\*e-mail: 2389683010@qq.com

hand, blasting-induced vibrations may cause structural damage and human discomfort [3–6]. On the other hand, the CO and NO<sub>x</sub> of post-blast fumes are the direct product of the detonation process. Exposure to these toxic gases can have a range of negative effects on the health and safety of exposed persons and on the surrounding environment [7, 8]. The NO<sub>x</sub> emissions during the use of AN explosives contaminate the local atmospheric environment of mining sites. Exposure to the high concentration of NO<sub>x</sub> can induce a number of chronic diseases, e.g., pulmonary oedema, acquired, or type II methemoglobinemia [9]. Attalla et al., [10] measured the concentrations of NO<sub>x</sub> by the mini-DOAS spectrometer and the values can reach between 5.6 and 580 ppm which was exceeding the safe limits [11]. Sincerely, the chemical reactivity of NO<sub>x</sub> can produce secondary pollutants, such as ozone, smog, and nitrate aerosols, by the chemical interaction [12, 13].

All of the above researchers pay attention to the blasting process of the open-cut coal mining because dozens to hundreds of tons of explosives are used each detonation and generally the orange/red cloud of NO<sub>2</sub> can be seen clearly. Although in the tunnel blasting operation fewer explosives are used per round, the CO and NO<sub>x</sub> are easier to accumulate in a confined space. Exposure of humans to these high concentrations can lead to injuries. Therefore General Administration of Quality Supervision [14], has made strict regulations on the monitoring of the concentration of CO, NO<sub>x</sub>, and other gases, so as to prevent excessive gas from causing harm to the human body.

To date, researchers have extensively studied on toxic fumes from underground blasting operations. Xu et al., [15] mentioned the impact of explosives on the environment in the study of greenhouse gas emissions of a highway tunnel. Huang et al., [16] suggested that the improvement of blasting efficiency and reduction of explosive consumption can remarkably reduce the environmental impacts. And the research mainly focuses on migration characteristics of blasting gases [17–19]. The methods for the control of gases in underground spaces are: prevention, extraction, isolation, containment and dilution. Dilution ventilation is one of the most effective control measures against blasting fumes and is universally applied [20, 21]. Toraño et al., [22] proved that the face ventilation effectiveness (FVE), or proportion of fresh air reaching the working face, ranges from 35% to 40% for a forcing ventilation system, whereas it ranges from 10% to 12% for an exhausting ventilation system. There are different algorithms to calculate gas clearance after blasting in development headings [20–24].

Considering the above mentioned studies, the CO and NO<sub>x</sub> of post-blast fumes are extremely harmful to production, human health, and the environment. And the research on pollution reduction is mainly about ventilation and migration characteristics. However, there are no suggestions on emission reduction from the source of gas generation. In other words, the researchers

can analyze emission characteristics from the blast model itself to reduce gas emissions. The NTNU, Swedish, and China models are the most widely used in the drill and blast tunnelling. Therefore, the original aim of this study to answer the following questions:

1. What are the emission characteristics of the three blast design models?
2. Which blast design model is the cleanest?

In order to identify the processes and inputs with the highest post-blast fumes impacts, this study build three blast design models based on one certain tunnel. To understand the emission characteristics of the blast design models, we then propose three indexes of total emission, emissions per area, and emission increment.

The paper was organized as follows, including this introduction. Section 2 introduced the research framework, blast design models, and evaluation indicators. Section 3 presented the main findings. Section 4 discussed the results in detail. Section 5 summarized the conclusions of the study.

## Materials and Methods

Fig. 1 presents the concepts and procedures of this research work. The general procedure for the research method consists of the following steps:

1. Through the existing experimental model of gas emissions, the emission per per unit charge is determined including emission of CO, NO<sub>x</sub>, and relative general toxicity.
2. The detailed blasting parameters of three models are put forward based on one certain 42.3 m<sup>2</sup> cross-section tunnel. And charge data of different functional zones, i.e., cut, stopping, lifter, and contour, are also acquired.
3. Put forward the evaluation indexes, i.e., total emissions, emission per area, and emission increments.
4. Calculate the gas emissions of three models through the above steps.
5. The emission characteristics of CO and NO<sub>x</sub> from three models are discussed and the cleanest blasting model is acquired.

### Mechanisms of CO and NO<sub>x</sub> Formation

There are many kinds of industrial explosives. Cardarelli [25] subdivided them into three main classes i.e., primary high explosives, secondary high explosives, and tertiary high explosives, according to the sensitivity of high explosives to detonation. The emulsion explosives discussed in this paper belong to the tertiary high explosives. The emulsion explosives are the most recent varieties of explosives used in underground tunnel excavation. Their basic components include oxidizing agents most common of which is ammonium nitrate (AN) [26].

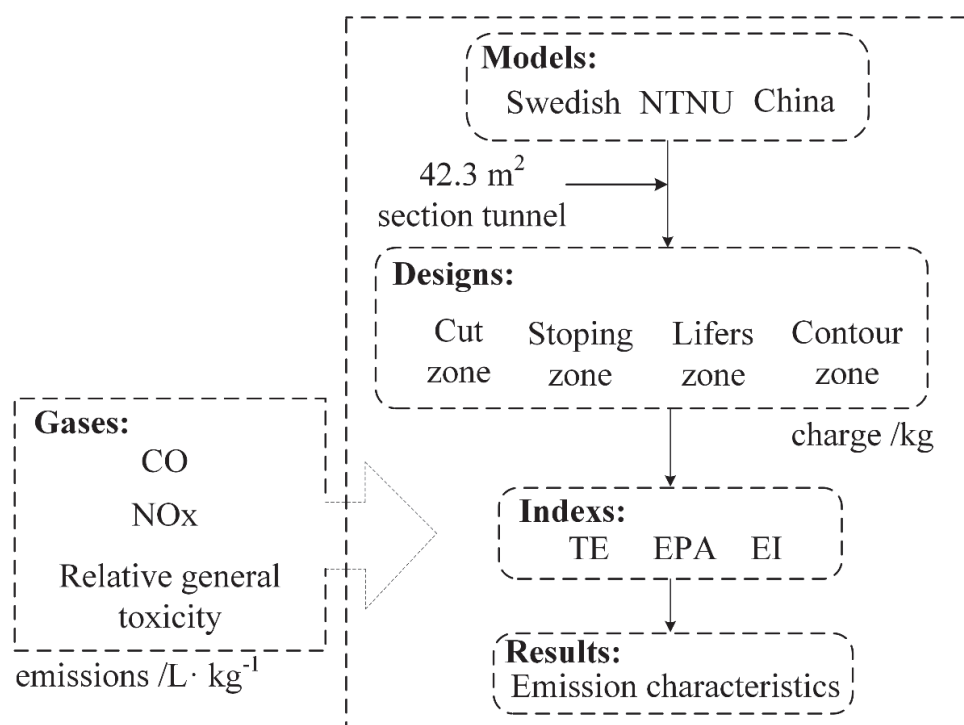
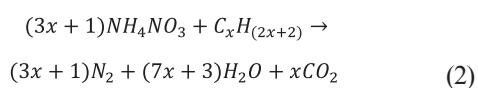


Fig. 1. Concepts and procedures of the research. TE, EPA, and EI indicate the total emissions, emission per area, and emission increments, respectively.

Most industrial explosives consist of four chemical elements, i.e., carbon, hydrogen, oxygen, and nitrogen. During the detonation process, gases evolve contain gaseous products, for example, carbon oxides, nitrogen oxides,  $N_2$ ,  $H_2$ , and  $H_2O$ , etc. Different products depend on “oxygen balance” (OB) which describes the reaction stoichiometry. It is calculated according to Equation (1), with the inclusion of metal term [27]:

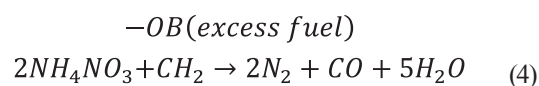
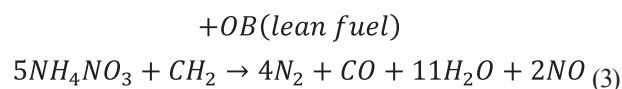
$$OB = \frac{16(O - 2C - \frac{1}{2}H - M)}{MW} \quad (1)$$

...where MW refers to the molecular weight in g mol<sup>-1</sup> of a compound (e.g., 80 g mol<sup>-1</sup> for  $NH_4NO_3$ ), the symbols O, C, and H correspond to the number of oxygen, carbon and hydrogen atoms, respectively, and M denotes the number of atoms of metal which is converted into metallic monoxide, MO. The OB value of the constituent component of an explosive mixture expresses the amount of oxygen atom, in mass fraction unit, in excess or deficiency with respect to stoichiometry. Cook and Talbot [28] proposed the zero oxygen balance in a general reaction as follows:



Water in emulsion explosives can affect the oxygen and prompt the formation of CO and NO. For example, nitric oxide can be generated by lean fuel (“oxygen positive”) explosives according to reactions similar to

(3) or carbon monoxide can be generated by excess fuel (“oxygen negative”) explosives according to reactions similar to (4):



The NO gas oxidizes rapidly in the atmosphere into orange-colored  $NO_2$ .



Furthermore, as shown in Fig. 2a), the interaction of fuel with AN under fuel-lean conditions leads to NOx species via the nitrous acid, nitro- and nitroso-hydrocarbon intermediates [29]. Sensitization of emulsion explosives with chemically-generated nitrogen bubbles (~400 mm in size) can also contribute to the emission of NOx. Fig. 2b) demonstrates the formation mechanism of NOx in the chemical gassing of emulsion explosives [29].

#### Study Purpose and Scope

The purpose of the study is to compare the emission characteristics of three blast models and acquire the cleanest model. The detailed blasting parameters of three models are put forward based on one certain

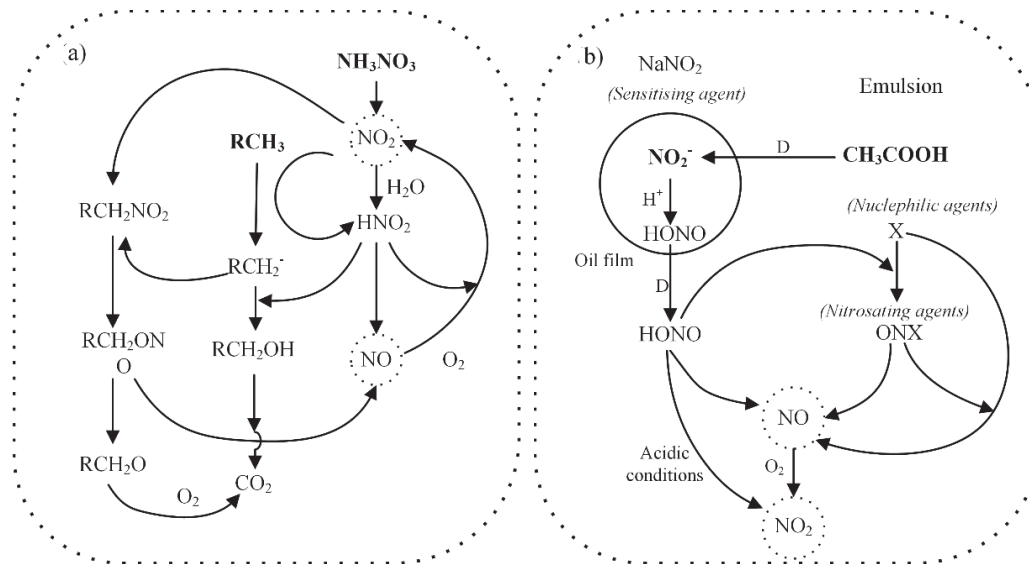


Fig. 2. The process of NOx formation.

42.3 m<sup>2</sup> cross-section tunnel which is presented by Zare & Bruland, [30].

The emulsion explosives are the most recent varieties of explosives used in underground tunnel excavation. Their basic components include oxidizing agents most common of which is ammonium nitrate (AN) [26]. It can also contribute to the emission of NO<sub>x</sub> and CO [29]. Each country applies its own rules and normative requirements for testing the content of toxic gases formed by the detonation of industrial explosives. Liu et al., [31] adopted the closed blast cartridge with the volume of 50 liters and 110 grams of emulsion explosives which are produced by six different manufacturers to analyze the composition of gases. The mean values of carbon oxides, nitrogen oxides, and general relative toxicity are used in this paper (Table 1).

Relative general toxicity (RGT) emissions are described using the following equation [26]:

$$L_{CO} = CO + 6.5 \times NO_x \quad (6)$$

...where CO is the amount of carbon monoxide per unit charge in L/kg. NO<sub>x</sub> is the number of nitrogen oxides per unit charge in L/kg.

### Case Study of Certain 42.3 m<sup>2</sup> Cross-Section Tunnel

#### Design of NTNU and Swedish Models

This section introduces the design of the NTNU and Swedish models. Swedish blast design model started with [32], and has been further developed afterward [33]. Persson et al., [34] published the complete blast design model and was later updated by Persson (2001). The tunnel face is divided into five separate sections i.e., cut, two stoping sections, contour, and lifter, as shown in Fig. 3.

The NTNU blast design model is described in the Project Report 2A-95 [30, 35]. Compared with the Swedish model, the tunnel face divides into the cut,

Table 1. The tests results of CO, NO<sub>x</sub>, and RGT emissions by LIU et al., (2010).

Tests number	Emulsion explosives			
	L <sub>CO</sub> /L · kg <sup>-1</sup>	V <sub>CO</sub> /L · kg <sup>-1</sup>	V <sub>NO<sub>x</sub></sub> /L · kg <sup>-1</sup>	L <sub>CO</sub> = CO + 6.5 × NO <sub>x</sub> /L · kg <sup>-1</sup>
1	362	25.7	0.17	26.8
2	366	35.9	0.55	39.5
3	364	28.4	0.59	32.2
4	356	19.9	3.85	44.9
5	354	24.6	0.61	28.5
6	356	29.7	1.32	38.3
Mean	360	27.4	1.18	35.0

stopping (easers), lifter (invert), row nearest contour and contour in the NTNU model. The design for each part should be determined by the following parameters in advance [30]:

1. Rock mass blastability.
2. Drill hole diameter.
3. Drill hole length.
4. Skill level of the tunnel crew.

In both models, the parallel hole cut with an empty hole(s) is used. Shokrollah Zare et al., [30] had introduced these two models in detail including the cut design, drilling pattern, charging, and look-out angle, etc. This paper will refer to these design parameters.

*Design of China Model*

However, Shokrollah Zare et al., [30] did not introduce the design of the China model. Therefore, the following will introduce it in detail. The tunnel face is divided into four sections, i.e., cut, easers (stopping), lifter, and parameter (contour), which is consistent with the other two models basically. The main difference is that the China model uses the V cut instead of a parallel hole cut.

*(1) Cut Holes*

At present, the tunnel blast design of railway, highway, or metro tunnels mainly adopts V cut in China. The V cut is designed according to its name and it has a symmetrical design. Cutting forms are mainly divided into single-stage and multi-stage V cut. And the multi-stage V cut e.g., 2-stage and 3-stage, etc, is widely used in engineering (Fig. 4). The determination of cutting forms is shown in Table 2.

The key technologies of the V cut are the following wang et al, [36]:

1. The angle of the V cut is related to rock mass and tunnel sections. Generally, the angle is 60°~75° and the spacing is 40~90 cm.
2. When the large tunnel cross-section adopts the V cut, the angle of first stage blastholes should be

decreased and the horizontal distance should be increased.

3. When the length of boreholes is greater than 2.5 m, a third of the bottom holes should be charged.
4. Uncharged length is 20% of the blastholes generally and not less than 40 cm.
5. V cut should be initiated by millisecond delay with a 50 ms interval among different stages.

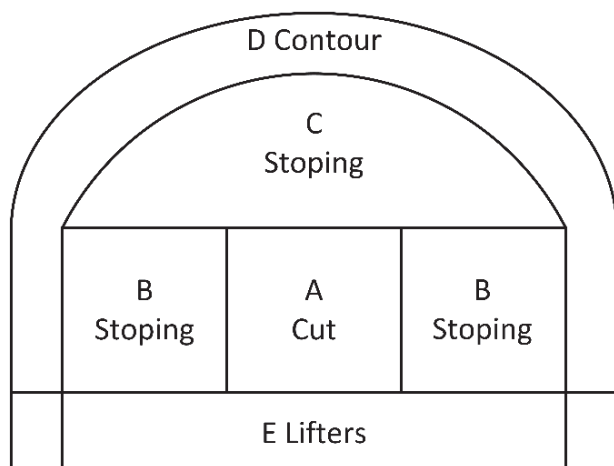


Fig. 3. Different tunnel sections of the Swedish model.

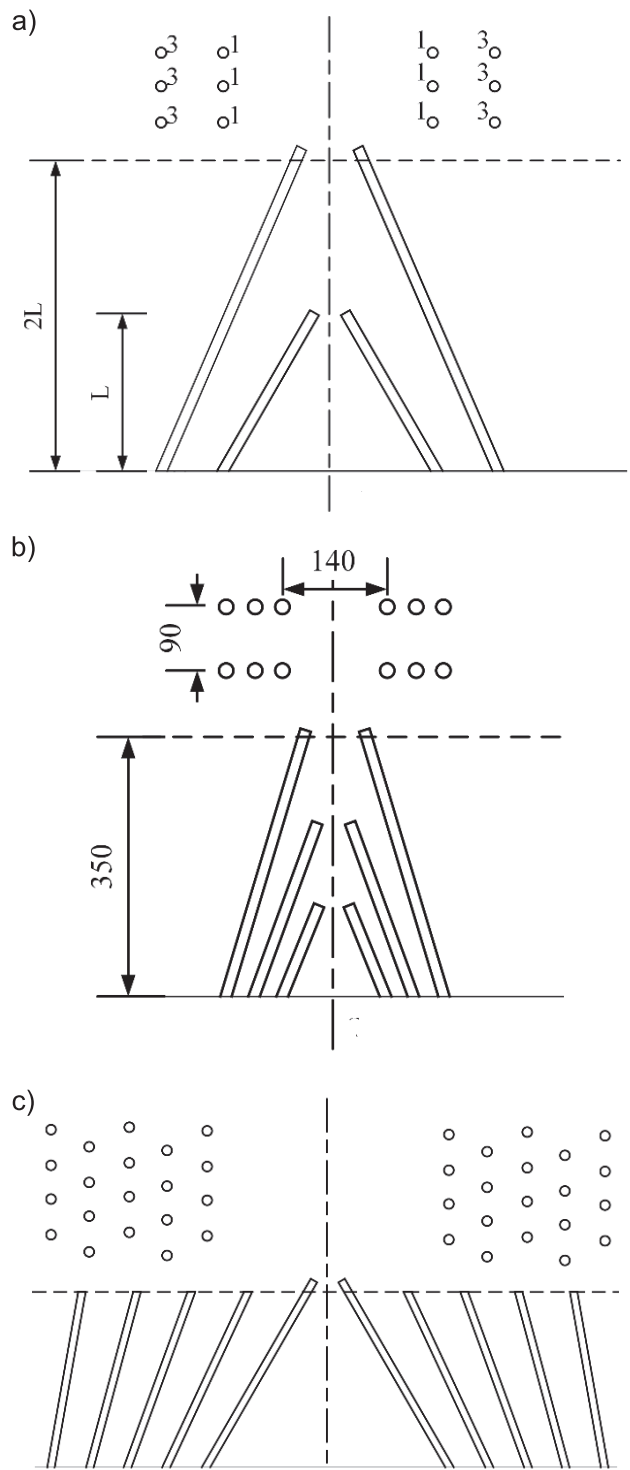


Fig. 4. Different cutting forms. a) 2-stage; b) 3-stage; 3) Multi-stage.

Table 2. Reference values of advance per round using V cut. Unit:m.

Cut type	Single-stage	2-stage	3-stage	Multi-stage
Moderately hard rock	1.5~2.0	2.0~3.0	2.5~4.0	>4.0
Hard rock	1.2~1.5	1.5~2.5	2.0~3.5	>3.0

### (2) Drilling Pattern

The spacing and burden of the lifter and stoping holes are related to rock mass mainly. The relationship between spacing and burden (S/B) is usually 1.25~1.70 [36]. The spacing of perimeter holes is generally using the following formulation:

$$[\sigma_t] \cdot S \cdot L \leq F \leq [\sigma_c] \cdot d \cdot L \quad (7)$$

$$S \leq [\sigma_c]/[\sigma_t] \cdot d \leq K_i \cdot d \quad (8)$$

...where  $\sigma_t$  is the tensile strength of rock (unit, Pa),  $\sigma_c$  is the compressive strength of rock, (unit, Pa), F is the explosion pressure (unit, N), d is the hole diameter (unit, m), E is the perimeter spacing (unit, m), L is the hole length (unit, m),  $K_i$  is the spacing ratio coefficient,  $K_i = [\sigma_c]/[\sigma_t]$ . The S also can be calculated using the following formula:

$$S = k \cdot d \quad (9)$$

$k = 10\sim 18$ , d is the hole diameter (unit, m).

The ratio between B and S is very important for a smooth blasting pattern. Wang et al, [36] suggested that the ratio of spacing to the burden of 0.8 is well.

$$B = 0.8 S \quad (10)$$

### (3) Charging

Different functional blastholes play different roles, and the charge amount of each kind of functional holes is also different. If smooth blasting is necessary, the charge of the lifter and stoping holes is adjusted

generally by charge coefficient. The calculation formula is as follows:

$$Q_i = q_1 L \varphi \quad (11)$$

$$q_1 = \frac{1}{4} \pi d_e^2 \rho_e \quad (12)$$

...where  $Q_i$  is the charge per hole (unit, kg),  $q_1$  is the linear charge concentration in kg/m, L is the borehole length in m,  $\varphi$  is the charge coefficient, as shown in Table 3,  $d_e$  is the borehole diameter in meters,  $\rho_e$  is the explosive density (unit, kg/m<sup>3</sup>). The charge of contour holes can be referred to the Table 4.

In engineering, tunnel crew usually adopt the decoupled charge which is a non-full charge along a borehole axis, i.e., the charge diameter is smaller than borehole diameter (Fig. 5b). And also while using the air deck (Fig. 5a), it can reduce the bottom damage of the holes due to changing energy distribution [37].

### (4) Firing Pattern

Firing pattern must be planned so that each hole or group of holes get as favorable confinement and throw conditions as possible. The general sequence is cut, stoping, row nearest the contour, contour, lifter, and finally corner holes of the lifter in NTNU and Swedish models. However, in the China model, there is a minor difference. The sequence is cut, stoping, lifter, and contour.

### Data Collection

Persson et al., [34] proposed an example of blast design using the Swedish model for a tunnel with

Table 3. Reference value of charge coefficient  $\varphi$ .

Blastholes name	V cut	Stoping	Lifter	Remarks
$\varphi\%$	85~93	62~80	82~85	Full-face

Table 4. Reference value of smooth blasting.

Classification	S/cm	B/cm	B/S	Linear charge concentration/kg · m <sup>-1</sup>
Hard rock	55~70	60~80	0.7~1.0	0.30~0.35
Moderately hard rock	45~65	60~80	0.7~1.0	0.20~0.30
Soft rock	35~50	40~60	0.5~0.8	0.07~0.12

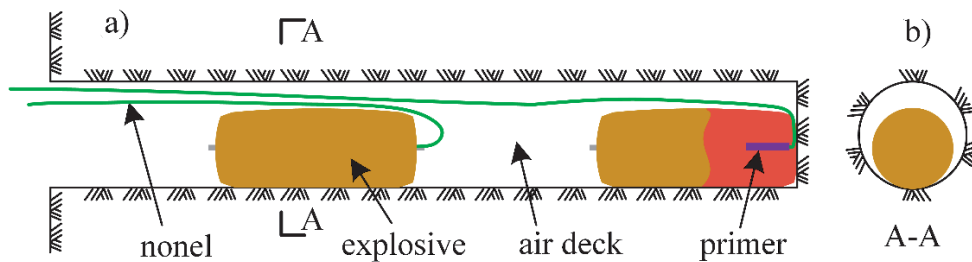


Fig. 5. The structure of the charge.

the 19.5 m<sup>2</sup> cross-section. Shokrollah Zare et al., [30] designed a blast pattern with the NTNU model based on the same tunnel cross-section. The main input of these two models are as follows:

1. Drillhole diameter = 45 mm.
2. Blasthole length = 3.2 m.
3. Empty hole diameter = 102 mm.
4. Explosive type = cartridge explosives.
5. Explosive density = 1200 kg/m<sup>3</sup>.
6. Rock constant = 0.4.

In this paper, the China model is redesigned with these parameters. It should be noted that the tunnel cross-section is enlarged in a certain proportion in order to adopt the V cut. The tunnel cross-section is changed from 19.5 m<sup>2</sup> to 42.3 m<sup>2</sup>. The rock constant  $C = 0.4$  is assumed to be equivalent to medium blastability [30] in this example. For the China model, the same input is used. For the Swedish and NTNU models, authors only increase several rows of perimeter blastholes based on the original design of Shokrollah Zare et al., [30] and Persson et al., [34]. The other parameters of holes, i.e., cut holes, stoping holes, and lifters, are still the same as the original design. Four-section cut burden is referred to the Table A.1. Shokrollah Zare et al, [30] offered the S/B relationship and burden values for the NTNU and Swedish models (Tables A.2~A.4). Finally, the authors put forward the detailed design parameters, as shown in Figs A.1~A.3.

The tunnel face of three design models is divided into four functional sections, i.e. cut zone, stoping zone, lifter zone, and contour zone. The cut zone refers to the part where the cutting holes are located, e.g., parallel holes or V cut holes. The stoping zone includes the horizontally breaking and downward breaking, i.e., sections B and C of Fig. 3. The row nearest contour of NTNU belongs to the stoping zone. The contour zone only refers to the part where the perimeter holes are located. The rest of the parts is defined as a lifter zone. The design parameters of different zones are shown in Tables A.5~A.7.

## Evaluation Indexes

### Total Emission

In order to compare the gas emissions of three models and acquire the cleanest model, this paper

proposes the index of the total emission. The CO, NOx, and RGT emissions of three models are calculated by the following equation:

$$U_{\text{gas}} = V_{\text{gas}} \times Q \quad (13)$$

...where  $U_{\text{gas}}$  is the CO ( $U_{\text{CO}}$ ), NOx ( $U_{\text{NOx}}$ ) and relative general toxicity ( $U_{\text{R}}$ ) emissions respectively in L,  $V_{\text{gas}}$  is the emissions per unit charge in L · kg<sup>-1</sup> (Table 1),  $Q$  is the charge of blast design in different zones (kg) (Fig. A.1~A.3). Therefore, the gas emissions of three blast design models are shown in Fig. 6.

### Emission Per Area

In the blast design model, the blastholes of four functional sections play different roles. For example, the cut zone provides space for the necessary expansion of the rock that will be blasted. And also different functional sections have different effects on the emission characteristics of the model. In order to explore the influence of functional blastholes on gas emissions, the emissions of the functional zone to its action area are taken as the index. The emissions per area are calculated by the following equation:

$$V_a = \frac{U_{\text{gas}}}{S_a} \quad (14)$$

...where  $V_a$  is the emissions per area in L · m<sup>2</sup>,  $U_{\text{gas}}$  is defined as the above,  $S_a$  is the action area in m<sup>2</sup>, i.e., area of tunnel section occupied by functional zones. The action area of each functional zone is shown in Table 5.

Table 5. The Area of different zones (unit: m<sup>2</sup>).

Function zones	Swedish model	NTNU model	China model
Cut	2.0	1.6	4.7
Stoping	20.1	22.7	21.6
Lifter	8.2	5.4	4.4
Contour	12.0	12.6	11.6
Total	42.3		

Emission Increment for Firing Pattern

With the processes of firing, the emissions of blast design models may change. These changes in emissions can be expressed in increments, which are the emission differences from the firing processes. This paper compared the emissions of three models in adjacent firing conditions. The comparison between the

emission of firing  $F_i$  and firing  $F_j$  was expressed as  $a_{F_i,F_j}$ ,  $i, j \in \{1, 2, 3, 4\} = \{I, II, III, IV\}$ ,  $i = j + 1$ . The comparison matrix among the firing sequence was as follows.

$$A = \begin{bmatrix} \phi & & & \\ a_{F_2,F_1} & \phi & & \\ & a_{F_3,F_2} & \phi & \\ & & a_{F_4,F_3} & \phi \end{bmatrix}$$

This paper defined ‘the relative distribution of firing processes in emission increment’, shown in Equation (15).

$$a_{F_i,F_j,m} = \frac{E_{F_i,m} - E_{F_j,m}}{E_{F_j,m}} \times 100\% \quad (15)$$

...where  $a_{F_i,F_j,m}$  represents the ratio of emission during the firing process of different models,  $E_{F_i,m}$  is the gas emission of firing  $F_i$  from model  $m$ ,  $E_{F_j,m}$  is the gas emission of firing  $F_j$  from model  $m$ ,  $m \in \{m1, m2, m3\} = \{\text{Swedish model, NTNU model, China model}\}$ . The relative contribution of each firing process from three models was shown in Table 6.

Results and Discussion

Gas Emissions Each Model

Fig. 6a) provides the CO emission data of different blast design models, i.e., China, NTNU, and Swedish models. The CO emissions of the three models are 3358 L, 5281 L, and 4107 L, respectively. The sequence of CO emissions is China<NTNU<Swedish. The dashed black line expresses the maximum emissions of different functional zones. And in the stopping zone, the CO emissions are the largest.

Fig. 6b illustrates NOx emissions data of different blast design models. The NOx emissions of the three models are 145 L, 227 L, and 177 L, respectively. Fig. 7c) illustrates RGT emissions data of different blast design models. The RGT emissions of the three models are 4298 L, 6759 L, and 5256 L, respectively. The emission law of NOx and RGT from three models is the same as the CO emission. The China model has fewer gas emissions than the other two models. The NTNU and Swedish models emit 1.57 and 1.22 times as much as the China model, respectively.

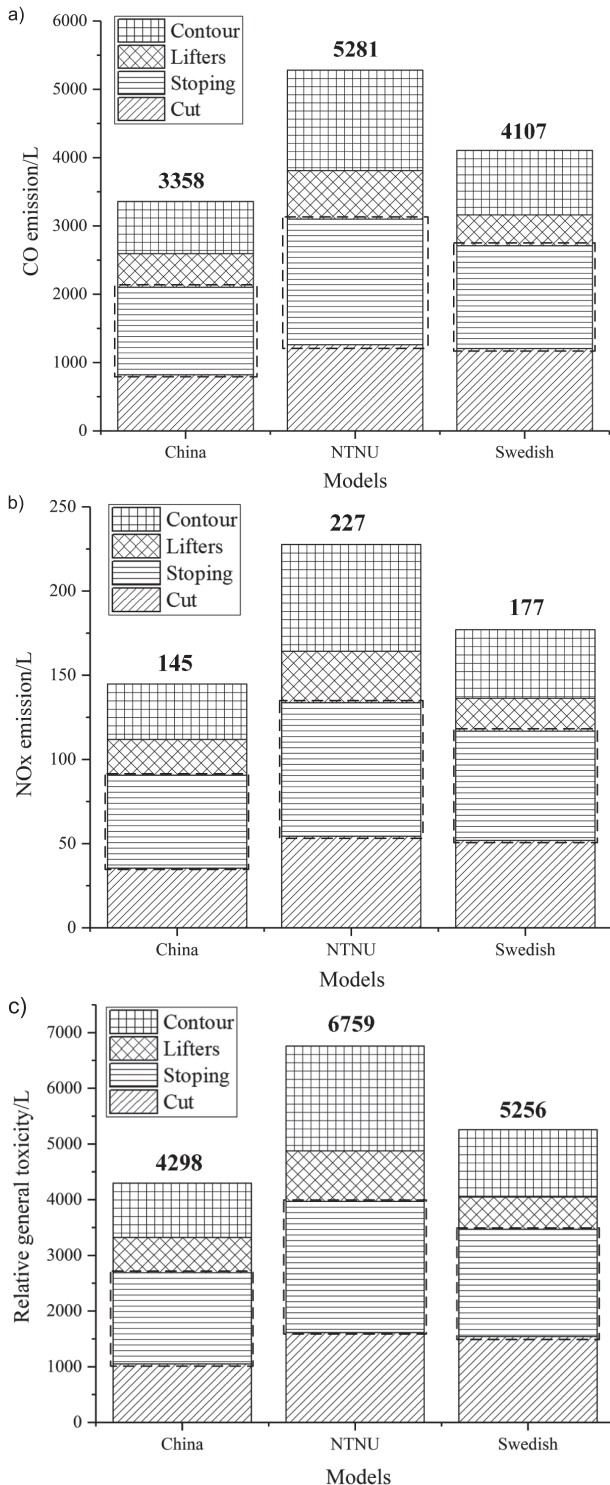


Fig. 6. CO, NOx, and RGT emissions of three blast models. a) CO; b) NOx; c) RGT.

Table 6. Relative emission distribution of firing processes.

$a_{F_i,F_j}$	Swedish model/ %	NTNU model/ %	China model/ %
$a_{F_2,F_1}$	25.0	45.8	-40.0
$a_{F_3,F_2}$	-37.2	-20.0	160.0
$a_{F_4,F_3}$	-52.3	-51.8	-40.4

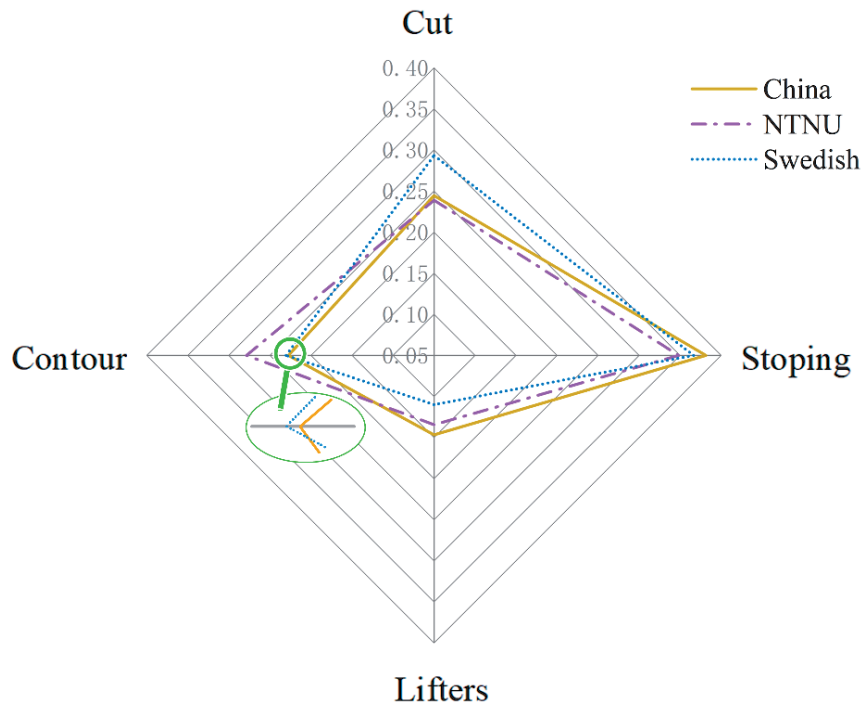


Fig. 7. The emission percentage of functional zones.

Fig. 7 reveals the emission percentage of functional zones, i.e., cut, stopping, lifter, and contour zones. In the China model, the sequence of emission percentage is stopping (38%) >cut (24%) >contour (23%) >lifter (15%). In the NTNU model, the sequence of emission percentage is stopping (35%) >contour (28%) >cut (24%) >lifter (13%). In the Swedish model, the sequence of emission percentage is stopping (37%) >cut (29%) >contour (23%) >lifter (11%). The emission percentage of stopping zone is the largest in all three models. And the emissions percentage of the lifter zone is the least. The emissions percentage of contour and cut zones is basically the same.

### Gas Emissions from Functional Zones

In order to illustrate the emissions of different functional zones in different design models, the emissions of the China model are used as a criterion. And the relative emissions of different zones of NTNU and Swedish models are shown in Fig. 8. In the cut zone, the sequence of emissions is NTNU (1.54) >Swedish (1.47) >China (1.00). In the stopping zone, the sequence of emission is NTNU (1.44) > Swedish (1.18) >China (1.00). In the lifter zone, the sequence of emission is NTNU (1.44) >China (1.00) >Swedish (0.92). In the contour zone, the sequence of emission is NTNU

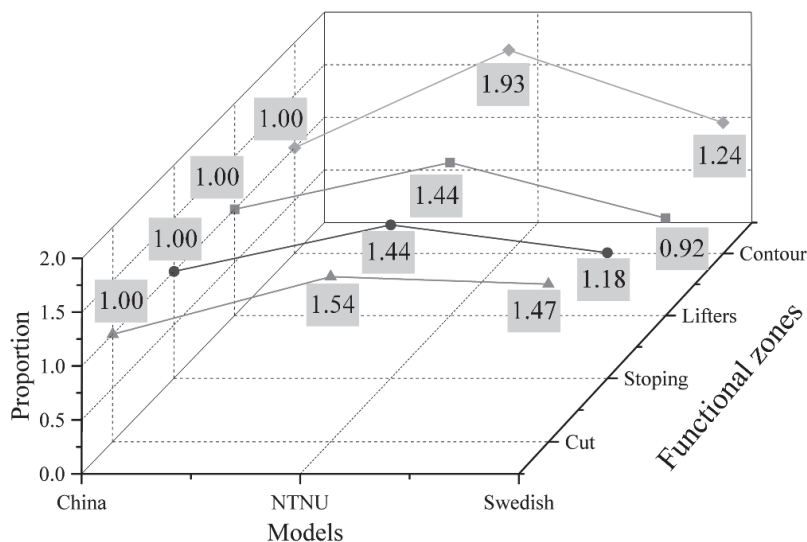


Fig. 8. Emissions comparison of functional zones from three models.

(1.93) >Swedish (1.24) >China (1.00). In all zones, the emissions of the NTNU model is the largest. Only in the lifter zone, the emissions of the China model are slightly larger than the Swedish model. But in the rest of the zones, the emissions of the China model is the least.

Fig. 9 shows the emission per area (EPA) of CO gas in different zones. In the China model, the total emissions of the cut zone are larger than the stoping zone. But, the emission per area presents the inverse relationship, i.e., cut zone ( $175 \text{ L} \cdot \text{m}^{-2}$ ) >stoping zone ( $59 \text{ L} \cdot \text{m}^{-2}$ ) (Fig. 9a). The NTNU and Swedish models

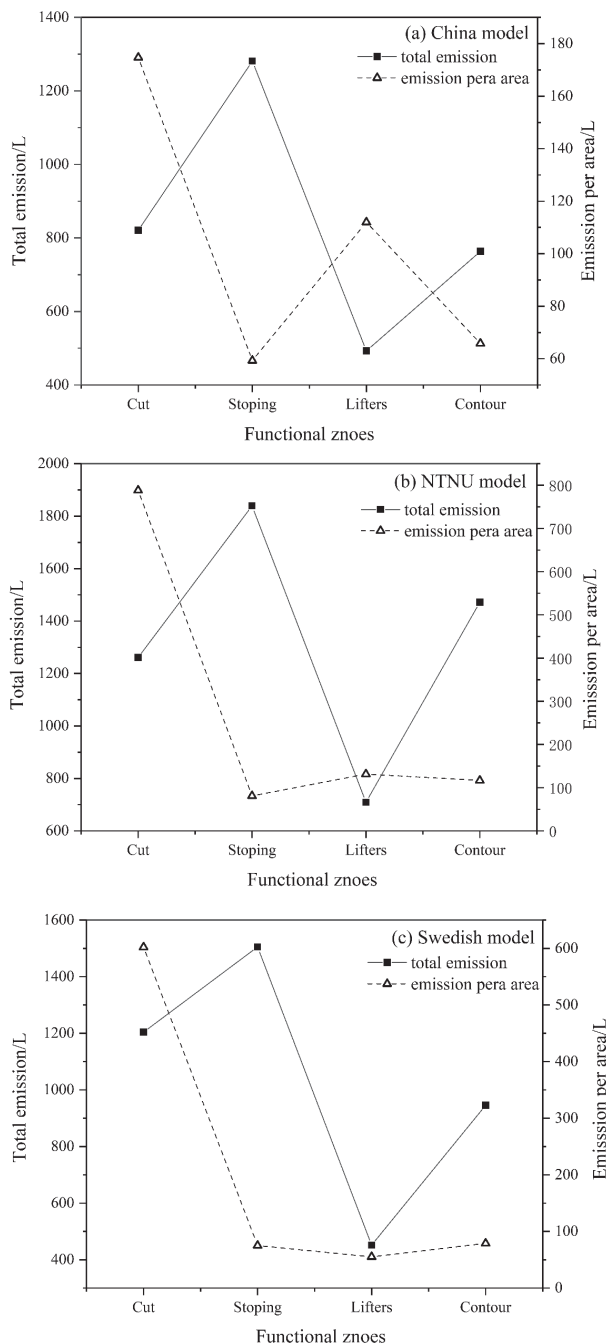


Fig. 9. Emission per area of CO of functional zones. a) China model; b) NTNU model; c) Swedish model.

also illustrate the same results (Figs 9b,c), e.g., cut zone ( $788 \text{ L} \cdot \text{m}^{-2}$ ) >stoping zone ( $75 \text{ L} \cdot \text{m}^{-2}$ ) in the NTNU model. The EPA of the stoping zone is the least in three models except the Swedish model in which the sequence is lifter ( $55 \text{ L} \cdot \text{m}^{-2}$ ) <stoping ( $75 \text{ L} \cdot \text{m}^{-2}$ ). Among the three models, the EPA of the cut zone is the largest. The EPA of the V cut ( $175 \text{ L} \cdot \text{m}^{-2}$ ) is lower than the parallel hole cut in which it is  $788 \text{ L} \cdot \text{m}^{-2}$  and  $602 \text{ L} \cdot \text{m}^{-2}$  in NTNU and Swedish models, respectively.

### Emission Transition Path

With the process of the firing, the amounts of gas emissions rose sharply. The CO and NOx emissions leap from the low emission level to a high level. Xu et al. [15] described the phenomenon as an “emission transition paths” in the study of GHG emission evaluation of tunnels. The relative contribution of each firing process from three models was shown in Table 7. Although the total emissions are increasing gradually during blasting, the relative increments of various firing processes may be negative. For example, the China model contributes -40.0% increment when the firing sequence changes from firing I to II, while the increment ratio of Swedish and NTNU models is 25.0% and 45.8% respectively. When the firing sequence changes from firing II to III, the increment ratio of NTNU, Swedish, and China models is -20.0%, -37.2%, and 160.0%, respectively. From firing III to IV, all three models contribute about -40%~50% increments. Consequently, in NTNU and Swedish models, the transition path is from positive increment to negative, and then to negative increment. However, in the China model, the transition path is from negative increment to positive, and then to negative increment.

### Discussion

#### Effect of Charge

The differences in blast model conditions determine the difference of charge, and the emissions of CO and NOx could also be changed. In brief, three factors, i.e., charge concentration, spacing, and burden, affect the charge of the blast models, thereby influencing the gas emissions. The NTNU model gives longer uncharged length than the Swedish model in stoping holes. However, in cut, lifter, and contour zones, the Swedish model has less charge than the NTNU model. Meanwhile, the Swedish model indicates a lower number of holes than the NTNU model due to the longer spacing and burden. Therefore, the Swedish model uses fewer explosives and produces fewer gases than the NTNU model. The China model not only designs the fewest linear charge concentration but also the highest spacing and burden values in the stoping zone. Ultimately, the emission sequence of NOx, CO, or relative general toxicity is China < NTNU < Swedish models.

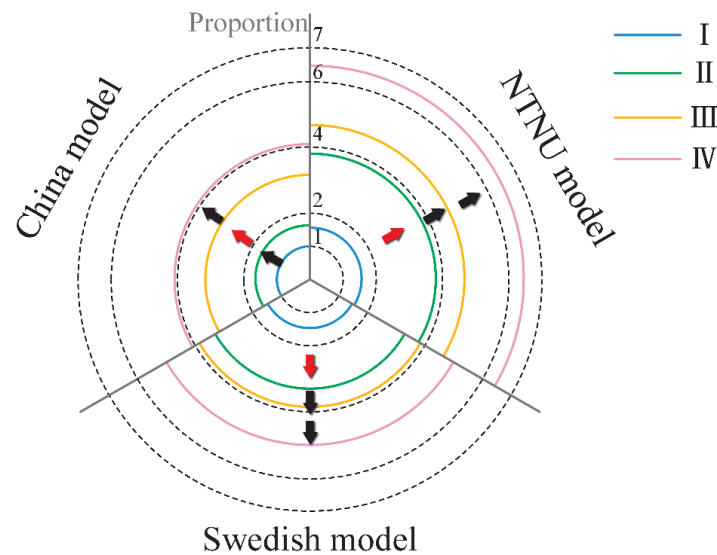


Fig. 10. Emission transition paths of three models. Note: The radiuses of concentric circles (arcs) are proportional to the emissions of functional zones. The emissions of the cut zone in the China model are used as the criterion. Red arrows indicate the positive emission increments, black arrows for negative value conversely. Roman numerals of I-IV represent the firing sequence.

#### *Effect of Functional Zones*

The stoping zone occupies nearly half of the cross-section for tunnel blasting (Table 6). And stoping zone gives higher explosives consumption. Therefore in three models, the emission percentage of the stoping zone is larger than other zones. The lifter holes which are located at the bottom contour of the tunnel give the lowest number of holes. And generally, the lifter holes are detonated after the cut and stoping holes. The existing opening gives enough expansion space for the lifter. Therefore, the lifter zone gives the lowest explosives consumption and emission percentage in three models.

The EPA value is better than the total emission value to reflect the blasting contributions of the functional zones. For example, the cut zone generally gives higher explosives consumption to provide space for the necessary expansion of the rock that will be blasted, e.g., stoping and lifter zones. However, the total emissions indicate that emissions of the cut zone are lower than the stoping zone. But the EPA of the cut zone is higher than the stoping zone, which indicates the contribution of the cut zone. Remarkably, The EPA of the V cut is lower than the parallel hole cut (Sect. 3.2). This is because the V cut requires fewer explosives and a larger blast area than the parallel hole cut. The EPA depends on the function of different zones. The contour holes control the smoothing of tunnel profile, e.g., overbreak and underbreak. Its blast design adopts the shorter spacing and burden than the stoping zone. Therefore, the EPA of the contour zone is higher than the stoping zone (Fig. 10). The rocks of cut and stoping zones are blasted in a heap near the lifter zone under the gravity. Therefore, the lifter zone needs to give

higher explosive consumption. And the EPA of the lifter zone is higher than stoping in China and NTNU models. However, in the Swedish model, the result is the opposite. This is because the spacing of lifter holes is too large in Swedish blast design [30].

Fig. 8 illustrates that the emissions of the stoping zone are the largest among the four functional zones in three models. In the stoping zone, the blast design of charge quantity and spacing is relatively flexible, e.g., the range of value is wider. It neither needs to increase the charge for expanding the space like the cut zone nor to reduce the spacing for controlling overbreak like the contour zone. Changing the design of cut and contour zones also may lead to blasting difficulties. Consequently, it is highly effective to control gas emissions by adjusting the charge and spacing of the stoping zone. Actually, we can see reductions in emissions when this paper adopts the stoping parameters of the China model.

#### *Non-Consistency of Emission Transition Path*

Fig. 10 illustrates that along with the processes of the firing, the discharge amount of function zones leaps from the low level to the high level in all three models. However, the transition paths are inconsistent in different models. This is determined by the characteristic of the firing patterns, actually. In NTNU and Swedish models, the firing pattern is cut, stoping, row the nearest contour, contour, lifter, and finally corner holes of the lifter. However in the China model, the firing pattern is cut, lifers, horizontally stoping, downward stoping, and finally contour blastholes. For example, the sequence from I to II, the CO emissions are 1204.2 L to 1505.3 L and 1261.2 L to 1839.2 L

in Swedish and NTNU models, respectively. In the China model, the CO emissions are 821.1 L to 492.6 L. Therefore, in NTNU and Swedish models, the emission increment is positive from I to II. On the contrary, the emission increment is negative in the China model.

### Conclusions

The originality of the work lies in comparing the emission characteristics of traditional blast design models, i.e., NTNU, Swedish, and China models, and acquiring the cleanest model. The authors proposed the indexes of total emission, emissions per area, and emission increment to compare the emission characteristics. The conclusions can be addressed as follows:

1) The China model gives the minimum explosive consumption due to the longest spacing, burden, and the lowest charge concentration of the blastholes. Therefore, the CO and NO<sub>x</sub> emissions of the China model are the least, followed by Swedish and NTNU models. Although the total emissions are different in different models, the emission percentage of different functional zones in each model is basically the same.

2) All in three models, the total emissions are dominated by the stoping zone. And emission percentage of the stoping zone is about 35%. The blast design of charge quantity and spacing of the stoping zone is relatively flexible. Therefore, it is highly effective to control CO and NO<sub>x</sub> emissions by adjusting the parameters of the stoping zone.

3) The EPA of V cut is lower than the parallel hole cut due to the V cut requires fewer explosives and a larger blast area. The emissions can increase along with the blasting process. However, the paths from the low emission levels to the high levels are usually inconsistent due to the characteristic of the firing patterns.”

### Acknowledgements

National Natural Science Foundation of China (Grant No. 71942006 and No. 51991395).

### Conflict of Interest

The authors declare no conflict of interest.

## Appendices A

Table A.1. Four-section cut burden and side length, m.

Quadrangle	Model	
	NTNU	Swedish
First quadrangle burden $B_1$	0.13	0.12
Second quadrangle burden $B_2$	0.16	0.16
Third quadrangle burden $B_3$	0.30	0.37
Fourth quadrangle burden $B_4$	0.55	0.62
Fourth quadrangle side length	1.25	1.42

Table A.2. S/B relationship.

Hole type	Model	
	NTNU	Swedish
Lifter	1	1
Stoping	1.2	1.25
Row nearest contour	1.1	-
Contour	~0.9	0.8

Table A.3. Burden values in meters for the NTNU model.

Hole type	Blastability	
	Good	Poor
Lifter	1	0.8
Stoping	1.15	1
Row nearest contour	1	0.9
Contour (average value)	0.8~1(0.9)	0.7~0.9(0.8)

Table A.4. Burden values in meters for the Swedish model.

Hole type	Explosive	
	ANFO	Cartridge explosive
Lifter	1.3	1.25
Stoping, horizontally breaking	1.2	1.1
Stoping, downward breaking	1.3	1.23
Contour (average value)	0.8~0.9 (0.85)	0.8~0.9 (0.85)

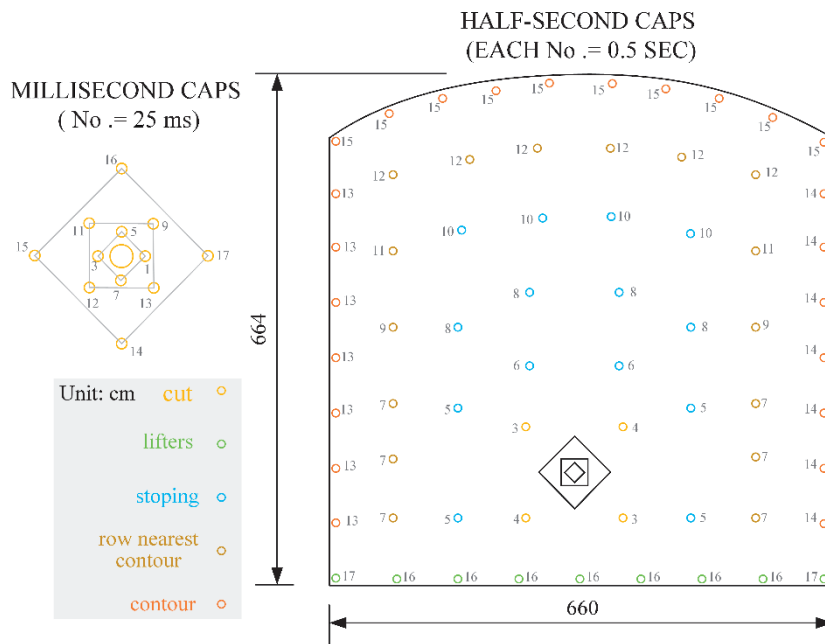


Fig. A.1 The NTNU blast design model.

Table A.5. The parameters of the NTNU blast design model.

Function zone	Delay period	Number of blastholes	Hole length/m	Charge per hole/kg	Total charge/kg
Cut	1,3,5,7,9,11~17 3,4 (ms)	16	3.2	2.88	46.08
Stopping	5~12 (s)	30	3.2	2.24	67.2
Contour	13~15 (s)	24	3.2	2.24	53.76
Lifter	16,17 (s)	9	3.2	2.88	25.92
Total	—	79	—	—	192.96

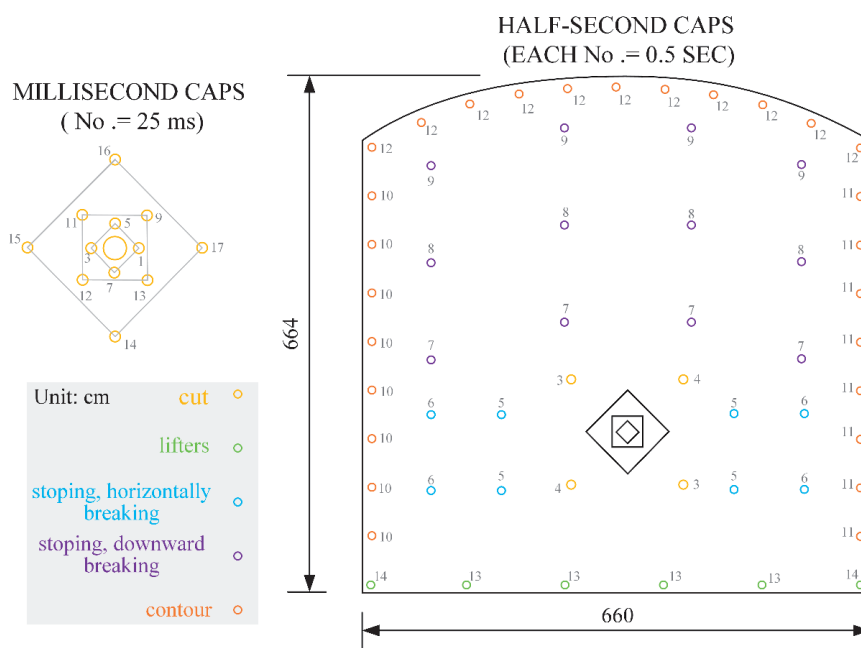


Fig. A.2. The Swedish blast design model.

Table A.6. The parameters of the Swedish blast design model.

Function zone	Delay period	Number of blastholes	Hole length/m	Charge per hole/kg	Total charge/kg
Cut	1,3,5,7,9,11~17 3,4 (ms)	16	3.2	2.75	44
Stoping	5~9 (s)	20	3.2	2.75	55
Contour	10~12 (s)	27	3.2	1.28	34.56
Lifter	13,14 (s)	6	3.2	2.75	16.5
Total	–	69	–	–	150.06

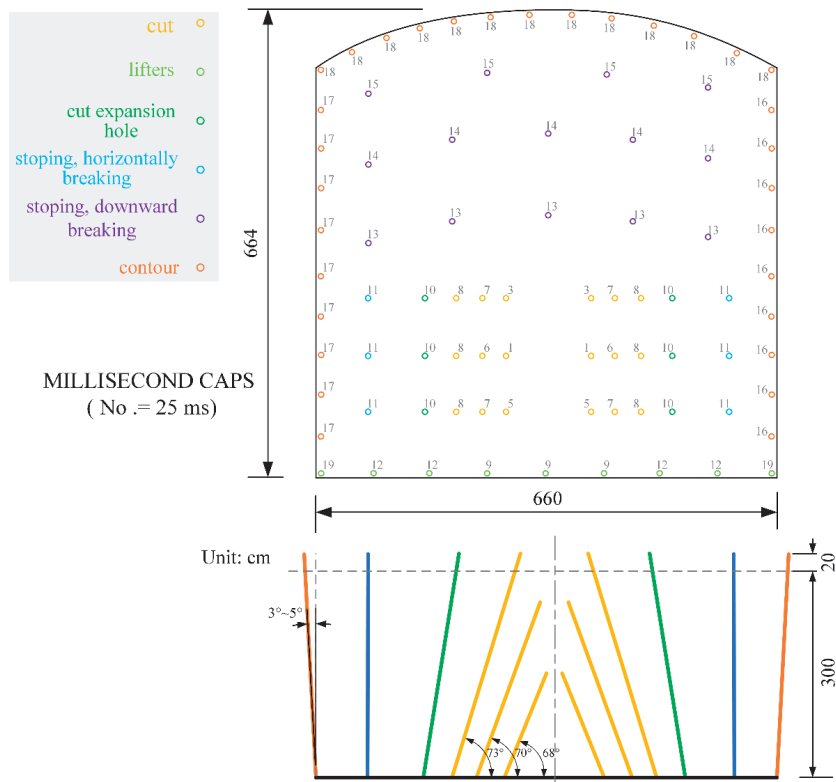


Fig. A.3. The China blast design model.

Table A.7. The parameters of the China blast design model.

Function zone	Delay period/ms	Number of blastholes	Hole length/m	Charge per hole/kg	Total charge/kg
Cut	1,3,5~8	18	1.5~3.2	1.0~2.3	30
Stoping	10,11,13~15	26	3.2	1.8	46.8
Contour	9,12,19	9	3.2	2.0	18.0
Lifter	16~18	31	3.2	0.9	27.9
Total	–	84	–	–	122.7

## References

1. FERREIRA C., FREIRE F., RIBEIRO J. Life-cycle assessment of a civil explosive. *Journal of Cleaner Production*, **89**, 159, 2015.
2. ZHAO Y., TIAN S. Data statistics of railway tunnel in China. *Tunnel Construction*, **37**, 641, 2017.
3. AVELLAN K., BELOPOTOCANOVA E., PUURUNEN M. Measuring, Monitoring and Prediction of Vibration Effects in Rock Masses in Near-Structure Blasting. *Procedia Engineering*, **191**, 504, 2017.
4. MOHAMED M.T. Performance of fuzzy logic and artificial neural network in prediction of ground and air vibrations. *International Journal of Rock Mechanics and*

- Mining Sciences, **48** (5), 845, **2011**.
5. NAVARRO TORRES V.F., SILVEIRA L.G.C., LOPES P.F.T., DE LIMA H.M. Assessing and controlling of bench blasting-induced vibrations to minimize impacts to a neighboring community. *Journal of Cleaner Production*, **187**, 514, **2018**.
  6. YAN Y., HOU X., FEI H. Review of predicting the blast-induced ground vibrations to reduce impacts on ambient urban communities. *Journal of Cleaner Production*, **260**, 121135, **2020**.
  7. ARAOS M., ONEDERRA I. Development of a novel mining explosive formulation to eliminate nitrogen oxide fumes. *Mining Technology*, **124** (1), 16, **2015**.
  8. HORÁK J., ŠIMANSKÝ V., AYDIN E., IGAZ D., BUCHKINA N., BALASHOV E. Effects of Biochar Combined with N-fertilization on Soil CO<sub>2</sub> Emissions, Crop Yields and Relationships with Soil Properties. *Polish Journal of Environmental Studies*, **29** (5), 3597, **2020**.
  9. WENG Z., MUDD G.M., MARTIN T., BOYLE C.A. Pollutant loads from coal mining in Australia: Discerning trends from the National Pollutant Inventory (NPI). *Environmental Science Policy*, **19-20**, 78, **2012**.
  10. ATTALLA M.I., DAY S.J., LANGE T., LILLEY W., MORGAN S. NO<sub>x</sub> emissions from blasting operations in open-cut coal mining. *Atmospheric Environment*, **42** (34), 7874, **2008**.
  11. LODGE J.P. Air quality guidelines for Europe. *Atmospheric Environment* (1967), **22** (9), 2070, **1988**.
  12. DENG W., LIU T., ZHANG Y., SITU S., HU Q., HE Q., WANG X. Secondary organic aerosol formation from photo-oxidation of toluene with NO<sub>x</sub> and SO<sub>2</sub>: Chamber simulation with purified air versus urban ambient air as matrix. *Atmospheric Environment*, **150**, 67, **2017**.
  13. JAFFE D.A., WIGDER N.L. Ozone production from wildfires: A critical review. *Atmospheric Environment*, **51**, 1, **2012**.
  14. LIBRARY W.P. General Administration of Quality Supervision, Inspection, and Quarantine, **2015**.
  15. XU J., GUO C., CHEN X., ZHANG Z., YANG L., WANG M., YANG K. Emission transition of greenhouse gases with the surrounding rock weakened – A case study of tunnel construction. *Journal of Cleaner Production*, **209**, 169, **2019**.
  16. HUANG L., BOHNE R.A., BRULAND A., JAKOBSEN P.D., LOHNE J. Environmental impact of drill and blast tunnelling: life cycle assessment. *Journal of Cleaner Production*, **86**, 110, **2015**.
  17. LIU Q., NIE W., HUA Y., WEI C., MA H., LIU C., ZHOU W. Study on Airflow Migration and Rock Dust Pollution Behavior in TBM Construction Tunnel. *Arabian Journal for Science and Engineering*, **45** (10), 8785, **2020**.
  18. XIU Z., NIE W., YAN J., CHEN D., CAI P., LIU Q., YANG B. Numerical simulation study on dust pollution characteristics and optimal dust control air flow rates during coal mine production. *Journal of Cleaner Production*, **248**, 119197, **2020**.
  19. MOEN A., MAURI L., NARASIMHAMURTHY V.D. Comparison of k-ε models in gaseous release and dispersion simulations using the CFD code FLACS. *Process Safety and Environmental Protection*, **130**, 306, **2019**.
  20. TORNO S., TORAÑO J., ULECIA M., ALLENDE C. Conventional and numerical models of blasting gas behaviour in auxiliary ventilation of mining headings. *Tunnelling and Underground Space Technology*, **34**, 73, **2013**.
  21. DE SOUZA E.M., KATSABANIS P.D. On the prediction of blasting toxic fumes and dilution ventilation. *Mining Science and Technology*, **13** (2), 223, **1991**.
  22. TORAÑO J., TORNO S., MENENDEZ M., GENT M., VELASCO J. Models of methane behaviour in auxiliary ventilation of underground coal mining. *International Journal of Coal Geology*, **80** (1), 35, **2009**.
  23. TORNO S., TORAÑO J. On the prediction of toxic fumes from underground blasting operations and dilution ventilation. Conventional and numerical models. *Tunnelling and Underground Space Technology*, **96**, 103194, **2020**.
  24. RODRÍGUEZ R., TORAÑO J., MENÉNDEZ M. Prediction of the airblast wave effects near a tunnel advanced by drilling and blasting. *Tunnelling and Underground Space Technology*, **22** (3), 241, **2007**.
  25. CARDARELLI F. A Concise Desktop Reference, **2018**.
  26. ZAWADZKA-MAŁOTA I. Testing of mining explosives with regard to the content of carbon oxides and nitrogen oxides in their detonation products. *Journal of Sustainable Mining*, **14** (4), 173, **2015**.
  27. AGRAWAL J.P. High Energy Materials. Wiley. Wiley, **2010**.
  28. COOK M.A., TALBOT E.L. Explosive Sensitivity of Ammonium Nitrate-Hydrocarbon Mixtures. *Industrial Engineering Chemistry*, **43** (5), 1098, **1951**.
  29. OLUWOYE I., DLUGOGORSKI B.Z., GORE J., OSKIERSKI H.C., ALTARAWNEH M. Atmospheric emission of NO from mining explosives: A critical review. *Atmospheric Environment*, **167**, 81, **2017**.
  30. ZARE S., BRULAND A. Comparison of tunnel blast design models. *Tunnelling and Underground Space Technology*, **21** (5), 533, **2006**.
  31. LIU L., NING P., LV C. Discussion on determination standard of toxic gas volume formed by detonation of industrial explosive. *Engineering Blasting*, **16** (1), 74, **2010**.
  32. LANGEFORS U., KIHLSSTRÖM B. The modern technique of rock blasting (3<sup>rd</sup> ed.). New York (N.Y.): Wiley. Retrieved from <http://lib.ugent.be/catalog/rug01:000198897> **1979**.
  33. LANGEFORS U., KIHLSSTRÖM B. The modern technique of rock blasting (3<sup>rd</sup> ed.). Stockholm: Awe/Gobers Wiley, **1978**.
  34. PERSSON P.-A., HOLMBERG R., LEE J. Charge Calculations For Tunneling. In *Rock Blasting and Explosives Engineering* (pp. 209-231). CRC Press, **2018**.
  35. JOHANNESSEN O. Project Report 2A-95 TUNNELLING – Blast Design, NTNU, **1995**.
  36. WANG X. Blasting Design and Construction. Metallurgical Industry Press Co., Ltd, Beijing, Beijing: Metallurgical Industry Press Co., Ltd. **2011**.
  37. HU S., FENG G., REN X., XU G., CHANG P., WANG Z., GAO Q. Numerical study of gas–solid two-phase flow in a coal roadway after blasting. *Advanced Powder Technology*, **27** (4), 1607, **2016**.